IIASA

International Institute for Applied Systems Analysis • A-2361 Laxenburg • Austria
Tel: +43 2236 807 • Fax: +43 2236 71313 • E-mail: info@iiasa.ac.at • Web: www.iiasa.ac.at

INTERIM REPORT IR-98-078/October

Optical Model of Atmospheric Aerosols in Russian Siberia for Correction of Satellite Data

Svetlana V. Petelina (pet@ionos.alma-ata.su)

Approved by
Sten Nilsson (nilsson@iiasa.ac.at)
Leader, *Forest Resources Project*

Foreword

Siberias forest sector has recently gained considerable international interest. IIASA, the Russian Academy of Sciences, and the Russian Federal Forest Service, in agreement with the Russian Ministry of the Environment and Natural Resources, signed agreements in 1992 and 1994 to carry out a large-scale study on the Siberian forest sector. The overall objective of the study focuses on policy options that would encourage sustainable development of the sector. The goals are to assess Siberia's forest resources, forest industries, and infrastructure; to examine the forests' economic, social, and biospheric functions; with these functions in mind, to identify possible pathways for their sustainable development; and to translate these pathways into policy options for Russian and international agencies.

The project has had difficulties accessing historical distribution of forest fires, insect infestations and disease outbreaks in the boreal forests of Russia. Similarly, spatial information on past forest harvest areas and on how general infrastructure development has influenced the forest structure is missing. Efforts are underway to establish a remote sensing system for the boreal forest zone (especially in Russia) that uses the most effective remote sensing data possible to fill-in missing historical disturbance information.

This paper discusses the optical parameters of the atmosphere in several areas of the Siberia region of Russia. These parameters are necessary for correct interpretation of remote sensing data in optical channels.

Contents

Abstract

Atmospheric components (aerosols and molecules) scatter and absorb solar radiation. They significantly influence the contrast and apparent resolution of satellite images of the Earth's surface taken in the visible and near infrared spectral channels. For accurate interpretation of satellite signals, remote sensing data have to be corrected for atmospheric effects. This requires knowledge of atmospheric spectral optical characteristics.

Aerosol components of the atmosphere vary in space and time. Accordingly to recent investigations, there can be a significant error in interpretation of optical satellite images when the spectral behavior of aerosol optical depth used in atmospheric correction procedures does not correspond to reality.

In this paper, an aerosol optical model that examines spectral optical depth and phase function for Siberia is presented. It is based on experimental measurements of the intensity of direct solar radiation, and on the microphysical parameters of aerosol submicron fractions. The model provides recent information on spectral behavior of aerosol optical parameters in Siberia and can be used with software for atmospheric correction of optical satellite data over Siberia forest areas.

Acknowledgments

The author is grateful to Professor Sten Nilsson and Alf Erik Öskog for useful comments and guidance during the summer 1998.

I would like to thank Dr. Gennadii G. Matvienko, Institute of Atmospheric Optics Siberian Branch RAS, Tomsk, Russia, for useful discussions and providing some experimental optical data for the Siberian region of Russia.

The author is also thankful to Michael Gluck for his editorial review of this paper.

About the Author

Dr. Svetlana V. Petelina is a Senior Scientist at the Department of Mathematical Problems of Remote Sensing, Space Research Institute, Almaty, Kazakhstan. Her areas of scientific interests include atmospheric correction of satellite optical data, inverse problems of atmospheric optics, modeling of aerosol optical and microphysical parameters, radiation transfer.

Space Research Institute, Ministry of Science-Academy of Sciences of Kazakhstan,

Shevchenko-15, 480100, Almaty, Kazakhstan

Email: pet@ionos.alma-ata.su

Phone: 7-3272-651-514, Fax: 7-3272-494-355

Optical Model of Atmospheric Aerosols in Russian Siberia for Correction of Satellite Data

Svetlana V. Petelina

1. Introduction

Satellite images of the Earth's surface are widely used for environmental applications, such as forestry, agriculture, land use, and ecology. Space-borne optical sensors measure the visible to short wave infrared spectrum originating from the solar radiation reflected from the Earth's surface and transmitted through the atmosphere. Atmospheric gases and aerosols scatter and absorb this radiation. They reduce the contrast and apparent resolution of surface features. For accurate interpretation, remotely sensed data in optical channels should be corrected for atmospheric effects.

The advantages of atmospheric correction are:

- Multi-temporal images may be compared and analyzed correctly.
- Images of different sensors may be compared and analyzed correctly.
- Spectral signatures of objects may be measured directly as reflectance or brightness temperature values.

Spectral reflectance signatures are necessary information for many advanced operational remote sensing applications such as:

- Environmental monitoring
- Harvest estimations in agriculture
- Forest management
- Forest damage monitoring
- Erosion monitoring
- Climate monitoring

Methods for atmospheric correction of satellite images are based either on the statistical approach or on simulations of satellite signals in the solar spectrum. The second procedure is more accurate and effective but requires spectral optical properties of the Earth's atmosphere (especially aerosol component) have to be known (Herman and Browning 1975).

The aim of this work is to estimate the optical characteristics of atmospheric aerosols in Russian Siberia in the visible and near infrared (NIR) spectral ranges. These aerosol characteristics can be implemented into the atmospheric correction software, and will provide more accurate interpretation of satellite data in optical channels.

2. Atmospheric attenuation of satellite signals

Under the assumption of a cloudless sky and a plane-parallel atmosphere, at each wavelength the radiance B measured by the satellite sensor with a narrow field of view can be expressed as the sum of the following components (Deschamps *et al*. 1980):

$$B=B_A+B_C+B_E$$

where B_A is the intrinsic atmospheric radiance, representing the radiance of light scattered from the direct sunbeam into the sensor's field of view by the atmosphere without reaching the surface (Figure 1 (a)).

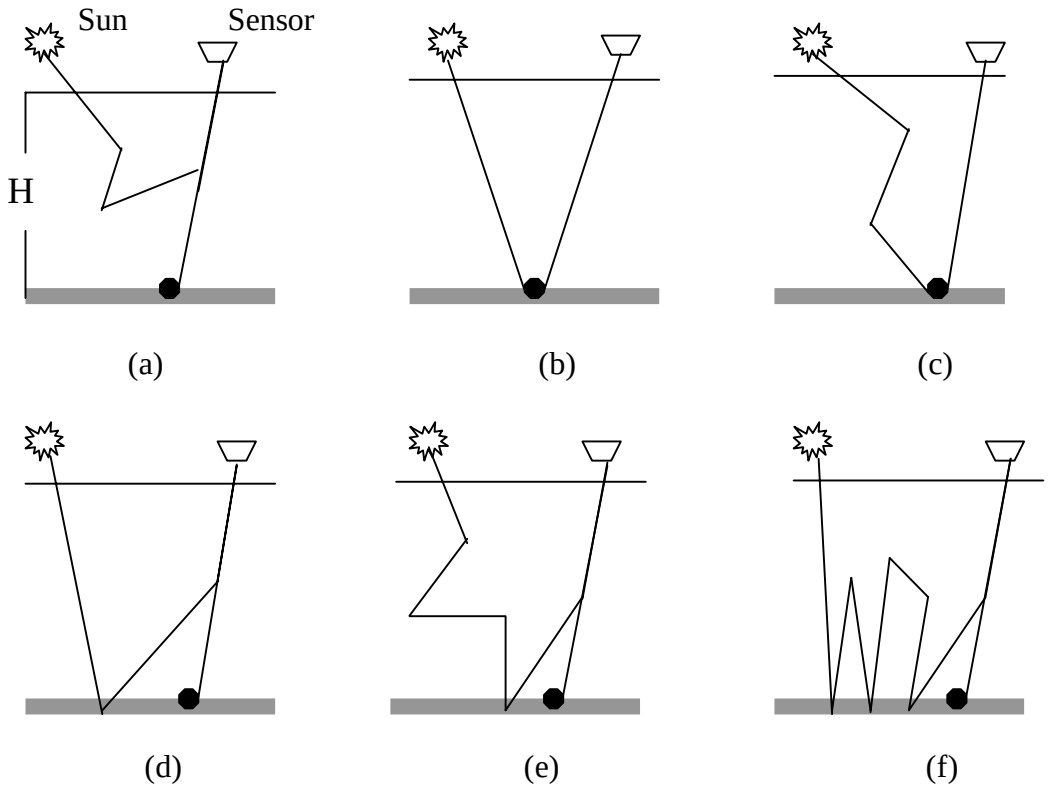

Figure 1. Components of sensor-measured radiance
of a terrestrial target (black point).

B_C is the radiance of light that is reflected only once from the target surface and then directly transmitted through the atmosphere into the sensor's field of view (Figures 1(b) and (c)). B_E is the radiance of light that is reflected by the Earth's surface surrounding the target (Figures 1 (d), (e) and (f)).

Numerous methods and algorithms have been proposed by various authors for estimating spectral values of radiance (B_A, B_C and B_E) and for removing these effects of the atmosphere from remotely sensed images (Kimes and Holben 1992, Rahman and Dedieu 1994, Singh 1992). These methods are based either on a statistical approach or on simulations of satellite signals in the solar spectrum. The latter approach is more accurate and commonly used. An example of the applying the atmospheric correction and haze removal procedures to LANDSAT TM image is shown on Figures 2a and 2b.

3. Basic principles of atmospheric correction procedure

Simulating the behavior of satellite signals in the solar spectrum is the main part of an atmospheric correction procedure. This method computes the solar radiation back-scattered by the atmosphere at the satellite altitude in different geometrical and optical conditions. It estimates the apparent reflectance at the top of the atmosphere for given surface spectral reflectance, solar and viewing zenith angles, sensor spectral response and atmospheric characteristics.

The algorithm of atmospheric correction, proposed by Zagolski and Gastellu-Etchegorry (1995), bases all intrinsic atmospheric radiance and average environment reflectance calculations on the numerical solution of the radiation transfer equation (Figure 3). The atmospheric parameters, which are variables in this equation, and therefore have to be known for atmospheric correction procedures, are described in section 3.1.

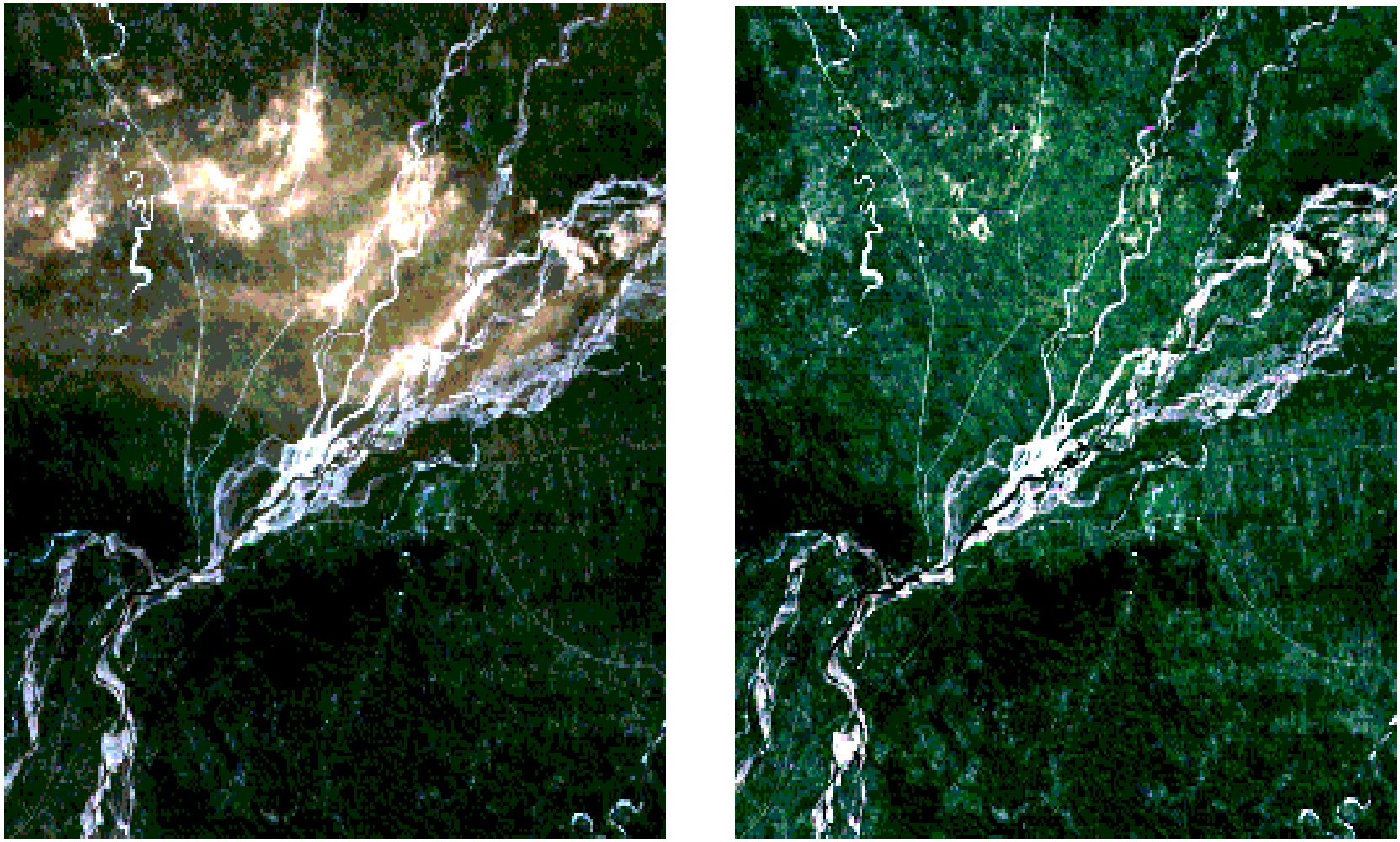

Before correction After correction

Figure 2a. LANDSAT TM imagery, color-composite (bands 1, 2, and 3) before and after atmospheric correction using ATCOR2 software.

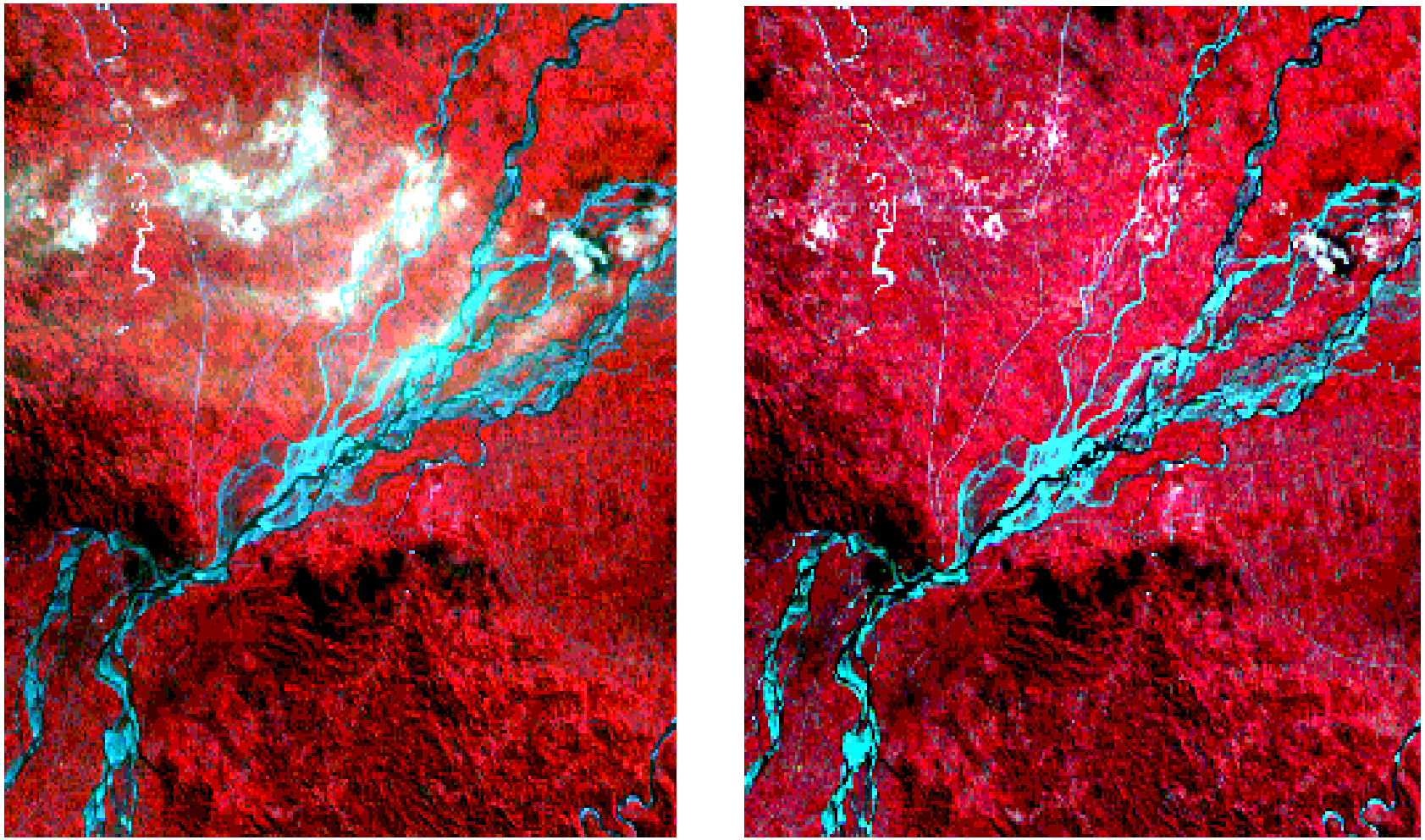

Before correction After correction

Figure 2b. LANDSAT TM imagery, color-composite (bands 1, 2, and 4) before and after atmospheric correction using ATCOR2 software

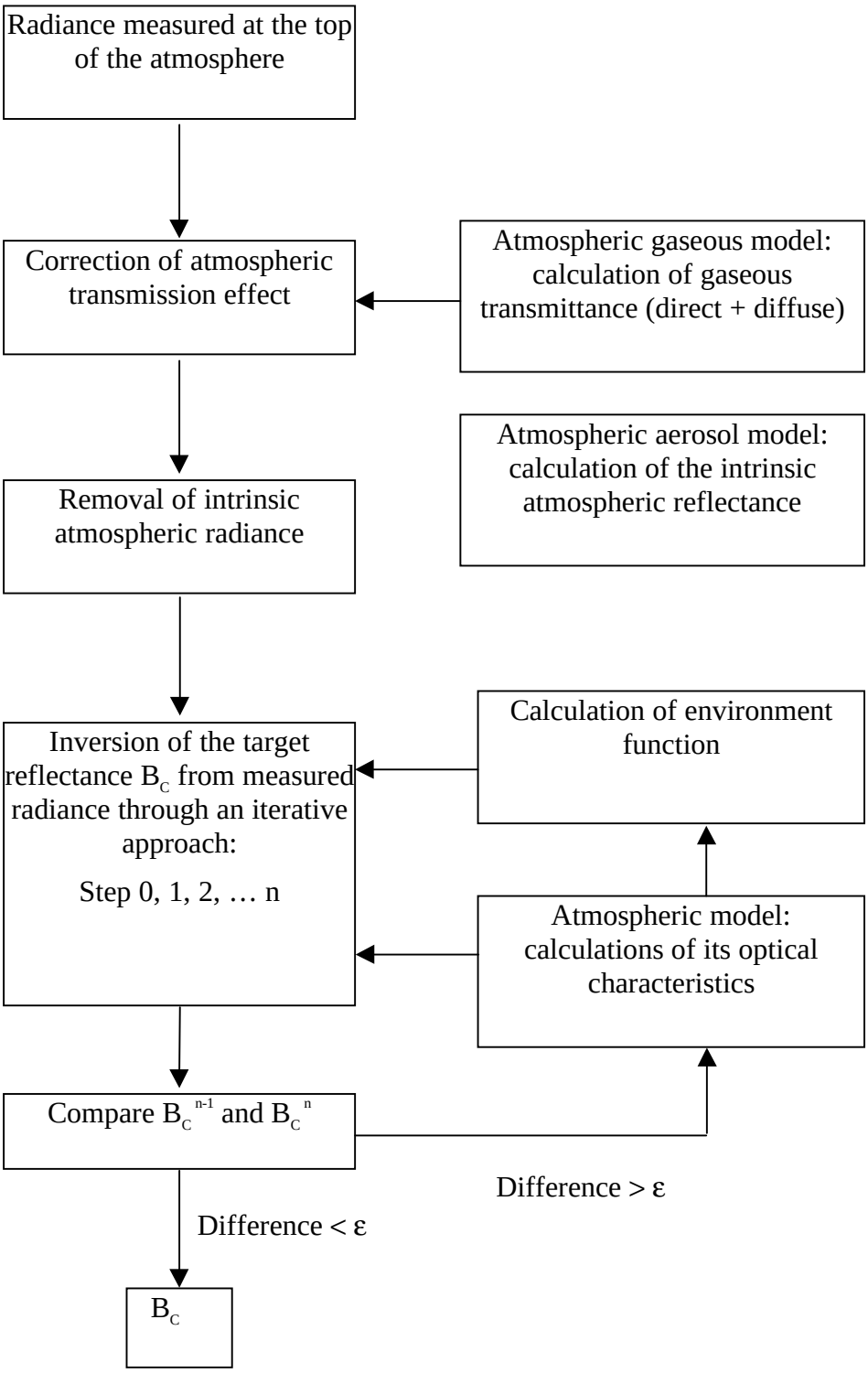

Figure 3. An atmospheric correction algorithm for remote sensing data.

3.1 Radiation transfer equation

The intensity of the solar radiation *I(r, s)* in some area of space with coordinates *r={x, y, h}* in the direction *s={z, ψ}* can be expressed as:

$$\hat{D}I = \hat{S}I + F_{\text{internal}} \tag{1}$$

with following boundary conditions:

$$\begin{cases} I\big/_{S\in\Omega^+} = \pi S_\lambda \delta(s - s_0), \\ I\big/_{S\in\Omega^-} = q\hat{R}I, \end{cases} \tag{2}$$

where *D* – operator of "transfer":

$$\hat{D} = \cos z \frac{\partial}{\partial h} + \sin z \cos\psi \frac{\partial}{\partial x} + \sin z \sin\psi \frac{\partial}{\partial y} + \sigma_{ext}(r); \tag{3}$$

S – integral of "impacts":

$$\hat{S}I = \sigma_{\text{scatt}}(r)\int_{\Omega} I(r, s')\mu(r, s, s')ds'; \tag{4}$$

R – operator of the "ground surface reflectance" under the assumption of the Lambertian surface:

$$\hat{R}I = \frac{1}{\pi}\int_{\Omega^+} I(x, y, H, s')\cos z' ds'; \tag{5}$$

F_{internal} – intensity due to internal sources of energy in the medium; σ_{EXT}, σ_{SCAT} – coefficients of atmospheric extinction and scattering respectively, μ - phase function of scattering, *q* – ground surface; $s_0=\{z_0, \psi_0\}$ – direction of the external solar radiation flux; *H* – the length of scattering medium in the *h* - direction; Ω^+, Ω^- - upper and lower hemispheres respectively; πS_λ - spectral solar constant.

For the plane-parallel, horizontally homogeneous atmosphere I(r, s)=I(z, s), and in visible and near infrared spectral ranges (where there is no internal sources of radiation) the radiation transfer equation (1) can be represented in a following form:

$$\cos z \frac{\partial I}{\partial h} + \sigma_{\text{ext}}(h)I = \sigma_{\text{scatt}}(h)\int_{\Omega} I(h, s')\mu(h, s, s')ds', \tag{6}$$

with the boundary conditions:

$$\begin{cases} I\big/_{S\in\Omega^+} = \pi S_\lambda \delta(s - s_0), \\ I\big/_{S\in\Omega^-} = q\frac{1}{\pi}\int_{\Omega^+} I(H, s')\cos z' ds' \end{cases} \tag{7}$$

3.2 Atmospheric optical characteristics — variables in radiation transfer equation

When sounding the Earth's surface from a satellite, the vertical profile of atmospheric scattering and absorption coefficients is not important, and coefficients of extinction and scattering can be substituted by the optical depth of extinction τ_{EXT} and scattering τ_{SCAT} of a whole atmosphere in the vertical direction. Spectral optical depth of the atmosphere with the height H is determined as:

$$\tau = \int_0^H \sigma(h)\, dh \tag{8}$$

Also, the atmospheric phase function can be presented as an average by height: $\mu(h,s,s') \rightarrow \mu(s, s')$. It can be determined from measurements of scattered radiation in the solar almucantar (when zenith angles of observational direction are equal to solar zenith angles) (Pyaskovskaya-Fesenkova 1957).

For numerical calculations of direct and diffuse solar radiation in the atmosphere (6), (7) it is necessary to know spectral values of the following atmospheric optical parameters:

- optical depth of extinction τ_{EXT},
- optical depth of scattering τ_{SCAT},
- averaged by height phase function μ.

Optical depth

For the each wavelength, atmospheric optical depth consists of the depth of aerosol scattering $-\tau_{A,\ SCAT}$, aerosol absorption – $\tau_{A,ABS}$, Rayleigh scattering – τ_R, and gaseous absorption – τ_{GAS} :

$$\tau_{EXT} = \tau_{A,SCAT} + \tau_{A,ABS} + \tau_R + \tau_{GAS} \tag{9}$$

Rayleigh scattering

Altitude dependence of the molecular (Rayleigh) scattering coefficient $\sigma_R(h)$ can be calculated by (Rayleigh 1871):

$$\sigma_R = \frac{8\pi^3 (n^2 - 1)}{3N\lambda^4} \frac{3(2+\Delta)}{6-7\Delta} \approx \frac{32\pi^3 (n-1)^2}{N\lambda^4} \frac{(2+\Delta)}{(6-7\Delta)} \quad , \tag{10}$$

where N(h) – molecular concentration (cm^{-3}); n(h, λ) – index of the air refraction; Δ - depolarization coefficient caused by the molecular anisotropy for atmosphere: for air Δ=0.042. Formula (10) was used to calculate altitude dependence of the molecular (Rayleigh) scattering coefficient $\sigma_R(h)$ at sea level for λ=0.503 μm (Table 1).

Table 1. Altitude dependence of $\sigma_R(h)$ at the normal atmospheric pressure for λ=0.503 μm.

h, km	σ_R, km^{-1}	h, km	σ_R, km^{-1}	h, km	σ_R, km^{-1}	h, km	σ_R, km^{-1}
0	1,69 -2	9	6,44 -3	18	1,68 -3	55	7,82 -6
1	1,53 -2	10	5,71 -3	19	1,44 -3	60	4,28 -6
2	1,39 -2	11	5,04 -3	20	1,22-3	65	2,25 -6
3	1,25 -2	12	4,31 -3	25	5,54 -4	70	1,14 -6
4	1,13 -2	13	3,67 -3	30	2,55 -4	75	5,51 -7
5	1,02 -2	14	3,14 -3	35	1,17 -4	80	2,55 -7
6	9,11-3	15	2,69 -3	40	5,52 -5	85	8,13 -8
7	8,14 -3	16	2,30 -3	45	2,71 -5	90	4,72 -8
8	7,26 -3	17	1,97 -3	50	1,40 -5	100	7,74 -9

Knowing the altitude dependence of $\sigma_R(h)$, one can calculate the Rayleigh optical depth for standard pressure and λ=0.503 μm using the relation (8):

$$\tau_R(P_{NORM},\lambda_{0.503})=0.098$$

For another wavelength λ_X the $\tau_R(\lambda_X)$ is calculating from the following relation:

$$\tau_R(\lambda_X)= \tau_R(\lambda_{0.503})\times(\lambda_X/0.503)^{-4}$$

For another atmospheric pressure P:

$$\tau_R(P, \lambda)= \tau_R(P_{NORM}, \lambda)\times P/P_{NORM}$$

Gaseous absorption

In the visible and NIR spectral ranges, τ_{GAS} is determined by the ozone component. Optical depth of ozone absorption $\tau_{OZ,}$ can be calculated using the total ozone content in the vertical column of the atmosphere X (DU), measured either at ground stations or from satellites:

$$\tau_{OZ}=\alpha X\ ln(10)$$

where α - decimal coefficient of ozone absorption (Table 2).

Table 2. Spectral values of α – the decimal coefficients of ozone absorption

λ, μm	0,405	0,446	0,503	0,550	0,647	0,710
$\alpha \cdot 10^3$, cm^{-1}	0	0	17,5	37,2	29,0	9,1

Optical depth of Rayleigh scattering and gaseous absorption, calculated using this formula for the Summer period at middle latitudes (Table 3).

Table 3. Optical depth $\tau_R + \tau_{GAS}$ for the summer period at middle latitudes

λ, μm	0.409	0.439	0.485	0.514	0.553	0.638	0.673	0.870	1.061
$\tau_R + \tau_{GAS}$	0.320	0.252	0.170	0.145	0.127	0.097	0.077	0.067	0.087

Some satellite sensors have spectral bands, which partly cover the areas of water vapor absorption. In this case, the water vapor total content has to be measured.

Aerosol optical depth

Aerosol optical depth τ_A can be calculated from the total optical depth τ when all other components of τ are known, and the total optical depth of the atmosphere can be calculated from measurements of the intensity of direct and diffuse solar radiation (Pyaskovskaya-Fesenkova 1957, Tverskoi 1962).

Aerosol optical depth is the most variable parameter in time and space. Even in cloudless atmospheric conditions, the value of aerosol optical depth may change up to 10-15 times during several hours. That is why present approaches to the atmospheric correction procedure are based on the retrieving τ_A for a given wavelength directly from the satellite image.

A method for such retrieval of τ_A was proposed by Kaufman and Sendra (1988). This method makes it possible to compute the aerosol optical depth, on a pixel by pixel basis, with the help of spectral measurements in the blue and/or the red spectral bands. Nevertheless, it assumes that some aerosol optical parameters – spectral optical depth of absorption, and phase function – are already known. That is why the regional optical models of aerosol have to be developed for those territories, which are monitored from space. These models will provide the spectral dependence of aerosol optical depth and phase function for the prevalent types of aerosol particles generated by ground surface and air mass circulation.

Phase function

The phase function of scattering $\mu(\varphi)$ is determined by the relative weight of molecular (Rayleigh) - $\mu_R(\varphi)$ - and aerosol - $\mu_a(\varphi)$ - components:

$$\mu(\varphi)\tau=\mu_R(\varphi)\tau_R+\mu_a(\varphi)\tau_{a,scat}, \quad (11)$$

and is normalized under the following condition:

$$2\pi\int_0^{\pi}\mu\ (\varphi)\sin(\varphi)d\varphi = 1 \quad (12)$$

Phase function of Rayleigh scattering $\mu_R(\varphi)$ is well-known (Rayleigh 1871):

$$\mu_R(\varphi) = 3(1 + \cos^2\varphi)/16\pi$$

Aerosol phase function can not be presented in an analytical form. Its spectral angular values depend on particle size distribution, chemical composition and numerical concentration.

Aerosol phase function can be obtained by two ways:

1. When microphysical parameters of particles are known (numerical concentration, chemical constants, and size distribution), then $\mu_a(\varphi)$ can be calculated using, for example, the Mie theory of scattering (Deirmendjan, 1969).
2. When microphysical parameters are not available, $\mu_R(\varphi)$ can be calculated from the angular distribution of scattered solar radiation (Petelina 1997).

The first approach can be applied for calculation of $\mu_a(\varphi)$ from previously measured aerosol microphysical parameters. However, for the whole atmosphere these parameters vary significantly with the height, making it very difficult to measure them simultaneously at all heights from ground to 40-60 km.

The second approach is more accurate for satellite-based remote sensing because it provides angular dependence of the averaged in space aerosol phase function of a cloudless atmosphere. Spectral values of $\mu_a(\varphi)$ can be extracted from the angular dependence of the intensity of scattered radiation measured in solar almucantar $I(\varphi)$ within the range of scattering angles $\varphi \div 2^0$-150^0. The methodology used for calculation of $\mu_a(\varphi)$, is based on the numerical solution of the radiation transfer equation in a plane-parallel, horizontally homogeneous atmosphere. It makes it possible to take into account multiple scattering of solar radiation, aerosol absorption, and average value of the surface albedo.

Minimal value of scattering angle φ, for which it is possible to measure $I(\varphi)$, is about $1^0 - 1.5^0$. Assumption of the plane-parallel atmosphere restricts the maximal value of the solar zenith angle z_0 to 75^0-78^0. The maximal value of the scattering angle φ is determined as $2z_0$. That is why our method (Petelina 1997) provides the extraction of aerosol phase function within the limit of scattering angles: $2^0 \le \varphi \le 150^0$.

Sensitivity of $I(\varphi)$ to variations of the aerosol phase function is determined by the wavelength and by the angle of scattering. For example, due to the prevalent Rayleigh scattering, $I(\varphi)$ is practically not sensitive to variations of $\mu_a(\varphi)$ in spectral range 0.4-0.5 μm at normal background aerosol content.

Therefore, the accuracy of the extraction of aerosol phase function $\mu_a(\varphi)$ from angular distribution of $I(\varphi)$ in the solar almucantar depends on the wavelength and scattering angle. This dependence have been estimated numerically (Petelina 1997) (Figure. 4).

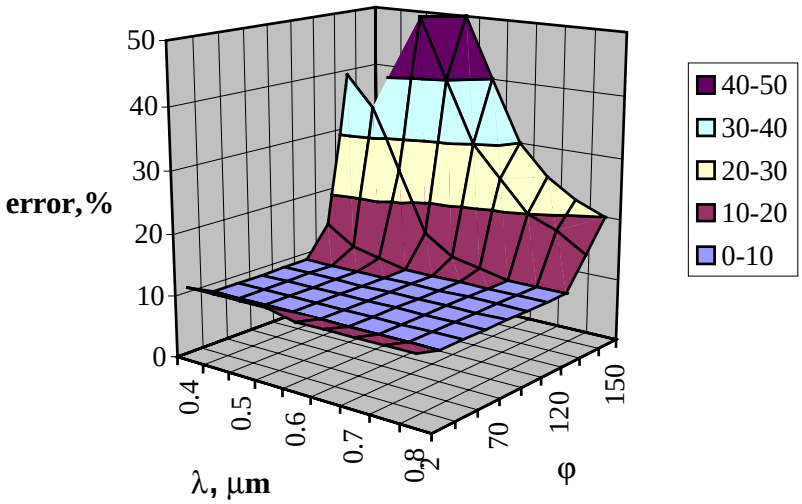

Figure 4. Spectral and angular dependence of the error of calculation of $\mu_a(\varphi)$ from $I(\varphi)$.

4. Experimental data on aerosol optical characteristics in Siberia region of Russia

Atmospheric transparency has been measured in different regions of Russia at several actinometric and ozonometric stations during last 20-25 years. The summary of these results made it possible to establish spatial distribution and long-period variations of aerosol optical depth (Guschin 1988). These measurements, however, have caveats such as aerosol optical depth was averaged for all the daytime, and measured only in a visible spectral range (λ=0.5 μm), and detailed measurements of aerosol optical depth τ_a conducted episodically and for restricted number of regions.

In Siberia, scientists from the Institute of Atmospheric Optics of the Siberian Branch of Russian Academy of Sciences, from the Siberian Physico-Technical Institute of the Tomsk State University, from the Institute of Physical Kinetics and Combustion (Novosibirsk) make such complex experiments on aerosol optical characteristics.

From 1992-1995 SATOR Program experimental field investigations focused on aerosol particle size spectrum, their concentration and chemical composition, because these parameters determine aerosol optical properties. Aerosol samples in Siberia have been collected from scientific stations of the Siberian Branch of Russian Academy of Sciences (Figure 5). As a result of these measurements, Koutzenogii, (1996) showed that in rural regions of Siberia, aerosol size spectrum corresponded to 3-modes Whitby distribution (Whitby 1975) for continental areas. The same study found aerosol size distributions were similar for Novosibirsk Oblast' and Baikal Lake region, which are separated by the distance about 1300 km. This result allows suggest that aerosols in Siberia have the same origin and therefore have similar optical characteristics in different rural Siberian regions.

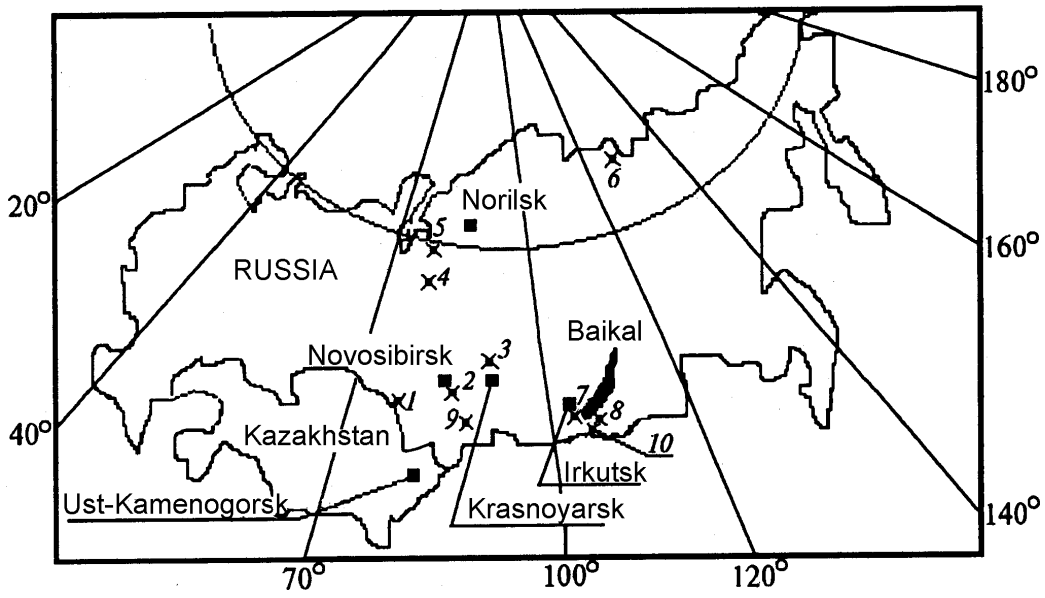

Figure 5. Geographic location of points (cross) for collection of aerosol samples in Siberia: 1-Karasuk, 2-Kluchi, 3-Pogorelskii Bor, 4-Tarko-Sale, 5-Samburg, 6-Tiksi, 7-Lystvyanka, 8-Tanhoi, 9-Ust-Kan, 10-Mondy.

4.1 Aerosol optical depth

The SATOR Program also provided the most recent systematic measurements of average, minimal and maximal values aerosol spectral optical depth in the Tomsk region in 1992-1995 (Table 3) and (Figure 6). Optical measurements were conducted using a multi-spectral solar photometer with 12 interference light filters in a spectral range 0.37 – 1.06 μm. Registration of data was in automatic regime with the duration 30 min every hour, and only for cases when Sun was not covered by clouds.

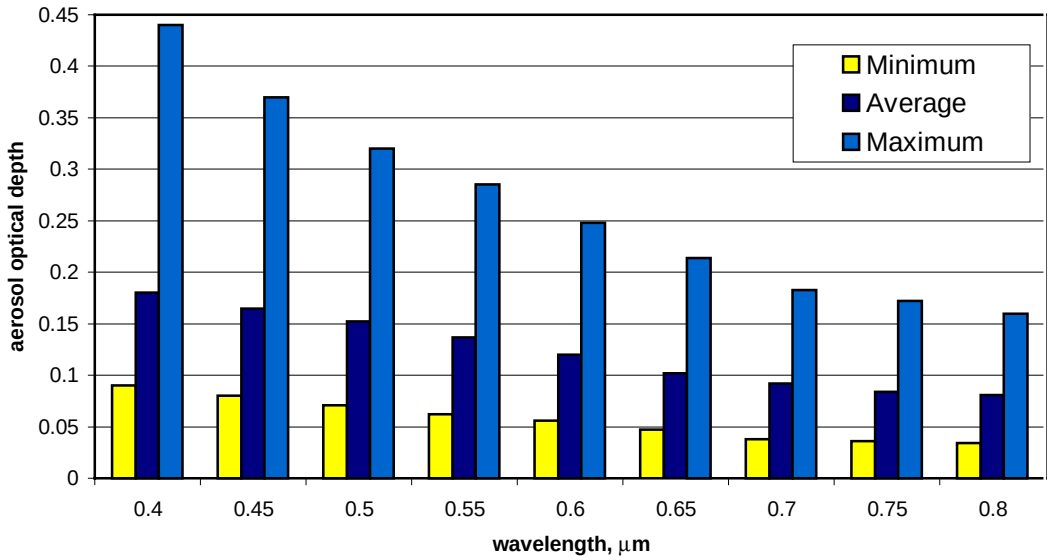

Figure 6. Average, minimal and maximal values of spectral aerosol optical depth measured during the Summer, 1994 in Tomsk region.

Recurrence of values of τ_a for λ=0.48 μm for all summer periods is presented in Fig. 7, where N - total number of cases, ΔN - number of cases for which values of τ_a are within definite interval. One can see that the most probable value of τ_a is: τ_a(0.48μm)=0.21, and more than 50% of τ_a are located within the area 0.12-0.24.

Seasonal and annual variations of aerosol optical depth

Statistical characteristics of aerosol optical depth (average τ_a^{aver}, minimal τ_a^{min}, and maximal values τ_a^{max}, and standard deviations α) measured for all seasons in Tomsk region in 1992-1995 are presented in Table 4 (Kabanov and Sakerin 1996).

Table 3. Statistical summary on the aerosol spectral optical depth τ_a measured in Western Siberia (Tomsk region) during 1992 – 1995 (Kabanov and Sakerin 1996).

Year and period	Number of days of measurements	Number of single series of measurements	Number of average (per hour) measurements
1992 23.05-30.07	52	1388	340
1992 05.12 - 22.12	8	105	21
1993 04.04 - 19.05	21	400	117
1993 22.05 – 13.06	20	503	176
1994 19.06 – 27.07	24	1126	148
1995 02.06 – 17.07	34	4272	187
Total amount	155	7864	989

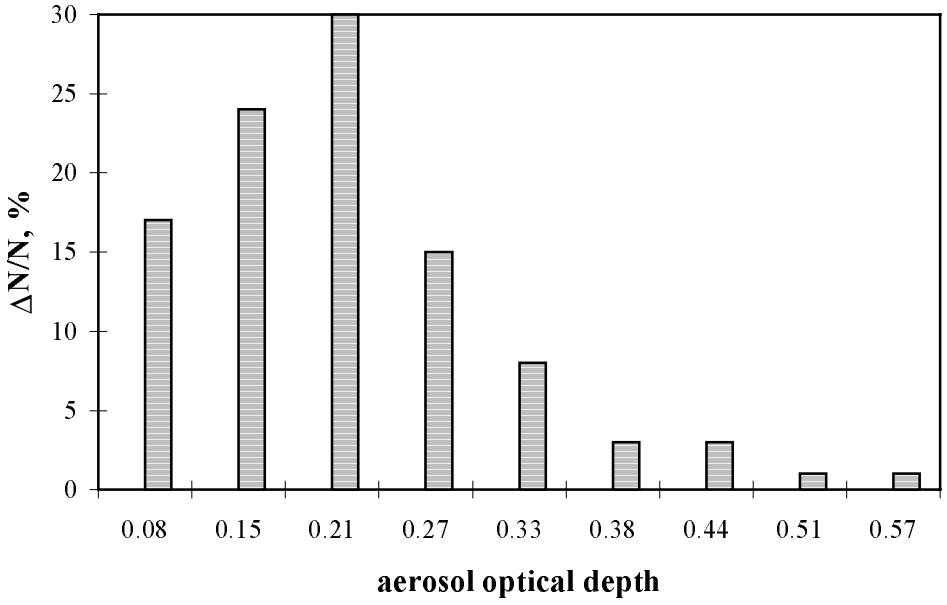

Figure 7. Recurrence of values of τ_a for λ=0.48 μm for all summer periods

Table 4. Statistical characteristics of aerosol optical depth (average τ_a^{aver}, minimal τ_a^{min},and maximal τ_a^{max} values, and standard deviations α) measured in 1992-1995.

		λ, μm						
		0.44	0.48	0.514	0.55	0.67	0.87	1.061
Summer 1992	τ_a^{aver}	0.284	0.260		0.215	0.163	0.117	
	α	0.094	0.085		0.068	0.052	0.040	
	τ_a^{max}	0.553	0.524		0.428	0.301	0.214	
	τ_a^{min}	0.138	0.133		0.105	0.066	0.045	
Winter 1992	τ_a^{aver}	0.233	0.238		0.222	0.189	0.173	
	α	0.083	0.081		0.075	0.01	0.065	
	τ_a^{max}	0.359	0.359		0.326	0.266	0.295	
	τ_a^{min}	0.095	0.101		0.092	0.082	0.079	
Spring 1993	τ_a^{aver}	0.260	0.239		0.204	0.147	0.110	
	α	0.118	0.107		0.095	0.074	0.065	
	τ_a^{max}	0.557	0.515		0.449	0.326	0.270	
	τ_a^{min}	0.091	0.087		0.063	0.048	0.024	
Summer 1993	τ_a^{aver}	0.282	0.249		0.190	0.147	0.129	
	α	0.136	0.122		0.090	0.07	0.045	
	τ_a^{max}	0.612	0.551		0.401	0.279	0.209	
	τ_a^{min}	0.092	0.082		0.057	0.037	0.028	
Summer 1994	τ_a^{aver}	0.164	0.146	0.131		0.086	0.064	0.060
	α	0.076	0.066	0.060		0.033	0.024	0.025
	τ_a^{max}	0.393	0.339	0.307		0.177	0.111	0.100
	τ_a^{min}	0.073	0.060	0.055		0.034	0.027	0.025
Summer 1995	τ_a^{aver}	0.176	0.155	0.146	0.133	0.100	0.074	0.058
	α	0.065	0.054	0.054	0.041	0.039	0.053	0.030
	τ_a^{max}	0.347	0.287	0.306	0.228	0.212	0.248	0.135
	τ_a^{min}	0.088	0.076	0.077	0.029	0.046		0.007

The observation data measured at Tomsk from 1992 to 1995 years (Table 4) are not appropriate for determining seasonal behavior of aerosol optical depth, because the duration of winter and spring measurements was very short, and autumn measurements were absent.

According to previous observations (Belan and Zadde 1988), there is a minimum of τ_a during the cold period of the year, and maximum - during the warm period. Also, the amplitude of seasonal variations of τ_a for different regions is about 0.1 and is not more than 0.15. Nevertheless, it possible to estimate the annual trend of τ_a for summer periods using the average, minimum and maximum values of $\tau_a(0.48)$ (and also standard deviation α) recorded in Tomsk for June 1992-1995 (for this month there is the largest amount of measurements every year) (Table 5).

Table 5. Average τ_a^{aver}, minimal τ_a^{min}, and maximal τ_a^{max} values, and standard deviations α of aerosol optical depth for λ=0.48 μm measured in June 1992-1995.

Year	τ_a^{aver}	α	τ_a^{min}	τ_a^{max}	Number of days
1992	0.261	0.059	0.178	0.404	19
1993	0.214	0.123	0.131	0.511	10
1994	0.191	0.071	0.114	0.339	10
1995	0.152	0.058	0.076	0.287	14

Decreasing values of aerosol optical depth as much as 60-70% from 1992 to 1995 can be explained by the absence of aerosol particles in the atmosphere after the eruption of the volcano Pinatubo in 1991.

Daily variations of aerosol optical depth

Variability of normalized values of aerosol optical depth τ_a^h/τ_a^{day} during the daytime for λ=0.48 μm is shown in Fig. 8 (Kabanov and Sakerin 1996). Values of τ_a^h were averaged for each hour.

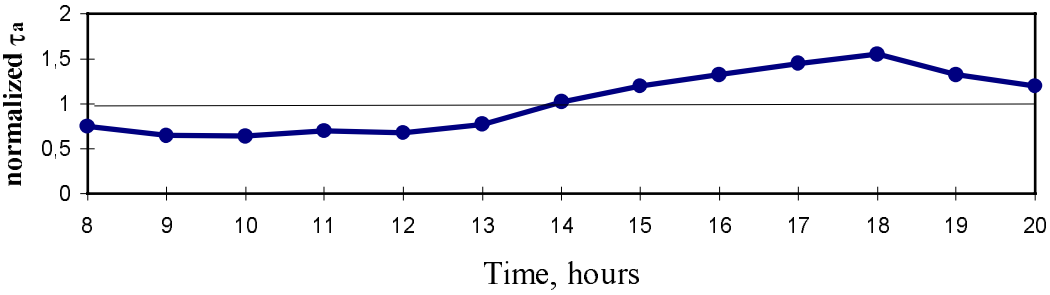

Figure 8. Normalized values of aerosol optical depth τ_a^h/τ_a^{day} during the daytime for λ=0.48 μm.

There are 3 zones in daily behavior of aerosol optical depth (Figure 8):

1. Morning period before 12 h – low values of τ_a^h with small variations.
2. Day period from 12 h to 18 h – continuos increasing of aerosol turbidity.
3. Evening period after 18 h – feebly marked decreasing of τ_a^h.

The maximum relative change of aerosol optical depth during these 3 periods is about 20%.

Dependence of aerosol optical depth on the air humidity

Accordingly to Pkhalagov *et al*. (1996), there is a strong dependency between values of aerosol extinction and the air humidity. Average aerosol coefficients of extinction at the ground layer, measured at the horizontal direction in background rural conditions near the forest zone, decrease as spectral wavelength increases (Figure 9). Also, increases in relative air humidity cause increased values of aerosol extinction coefficients. This means that spectral dependence of aerosol extinction coefficients remains constant during this process; changing in absolute values of extinction coefficients does not cause significant changes in their spectral behavior.

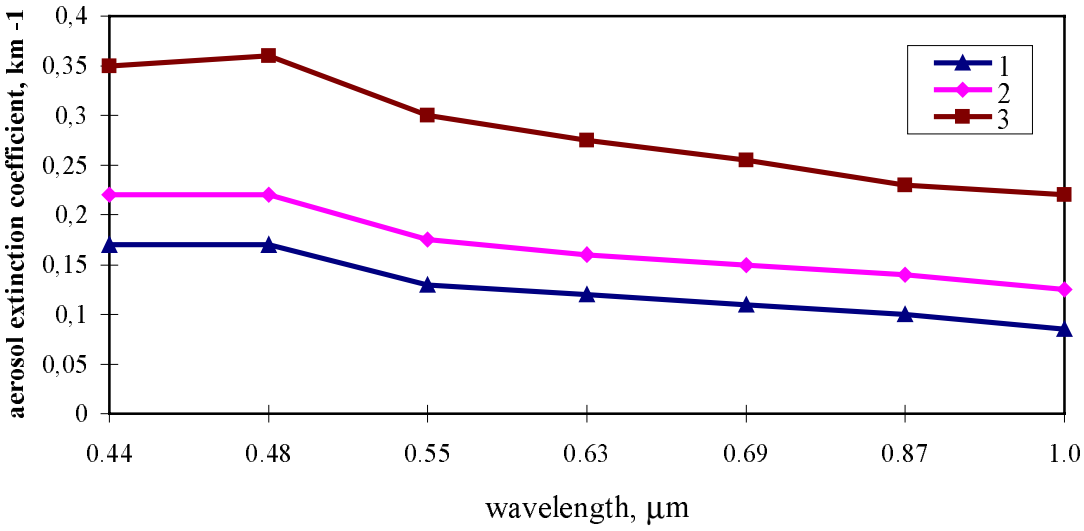

Figure 9. Spectral dependence of average aerosol extinction coefficients in Siberia rural area (Ob' river, 80 km from Tomsk) for different values of the relative air humidity. The three curves correspond to different values of the relative air humidity R: R=63 (curve 1), R=80 (curve 2), and R=96 (curve 3).

4.2 Aerosol phase function

As mentioned earlier, aerosol phase function can be calculated either from measurements of diffuse sky radiation in solar almucantar (Petelina 1997), or from known values of microphysical parameters of aerosol particles using, for example, Mie theory of scattering (Deirmendjan 1969). Weather conditions in Siberia (strong winds,

cloudy sky, and unstable optical transparency) make it difficult to measure the intensity of diffuse radiation in solar almucantar, especially for zenith angles more than 60^0. Some experimental data were obtained in the 1970s, however they are outdated and can not be considered as statistically representative. Therefore, aerosol phase function for Siberia must be calculated from measured values of microphysical parameters of aerosol polydisperse ensemble: particle size distribution and complex index of refraction for each fraction.

Many of the aerosol microphysical and optical parameters (especially for the submicron fraction) have been measured in different parts of Siberia since the 1960s by several groups headed by M.V. Panchenko, K.P. Koutcenogii, Ju. A. Pkhalagov, S.M. Sakerin, and others.

According to their results (Krekov and Rakhimov 1982, Koutzenogii 1996), aerosol optical and microphysical parameters in Siberia are similar to ones obtained by different authors for other continental regions of the Northern Hemisphere. Elements of the aerosol matrix of scattering were calculated using microphysical parameters of aerosol ensemble measured during several complex experiments in continental rural (background) areas (Krekov and Rakhimov 1982).

Using these results, we have calculated angular values of the aerosol phase function of scattering and their parameters of asymmetry for several wavelengths in visible and near IR spectral zones.

The parameter of asymmetry γ is important for the estimating the relative role of large and submicron aerosol particles in the scattering process. This parameter is determined from the following expression:

$$\gamma = \frac{\int_0^{\pi/2} \mu(\varphi)\sin(\varphi)d\varphi}{\int_{\pi/2}^{\pi} \mu(\varphi)\sin(\varphi)d\varphi}$$

We calculated vertical profiles of spectral aerosol phase function $\mu_a(\varphi)$ and their parameters of asymmetry γ for Northern continental regions for wavelengths λ: 0.530 μm, 0.694 μm and 0.860 μm (Tables 6, 7 and 8 respectively).

Table 6. Vertical profiles of spectral aerosol phase function $\mu_a(\varphi)$ and their parameters of asymmetry γ for Northern continental regions for λ= 0.530 μm.
Phase functions are normalized under the condition (12).

	φ									
h, km	0^0	1^0	5^0	10^0	15^0	30^0	70^0	90^0	100^0	110^0
0	73.5	33.3	1.83	0.843	0.592	0.255	0.031	0.014	0.011	0.009
1	52.1	29.3	2.47	0.948	0.616	0.243	0.028	0.012	0.010	0.008
2	31.4	21.9	2.33	0.845	0.558	0.241	0.036	0.015	0.013	0.010
3	20.2	16.2	2.29	0.784	0.497	0.235	0.042	0.021	0.016	0.013
4	18.2	14.3	2.05	0.775	0.516	0.247	0.043	0.021	0.016	0.013
5	16.5	12.9	1.88	0.779	0.535	0.254	0.043	0.021	0.017	0.014
6	14.9	11.4	1.74	0.788	0.554	0.261	0.043	0.022	0.017	0.014
7	9.93	7.70	1.54	0.764	0.555	0.270	0.045	0.023	0.017	0.015
8	6.56	5.23	1.35	0.735	0.552	0.277	0.047	0.024	0.018	0.015
9	4.37	3.61	1.17	0.704	0.541	0.281	0.049	0.025	0.019	0.016
10	2.00	1.88	0.95	0.660	0.534	0.287	0.052	0.026	0.020	0.017
11	3.36	3.13	1.31	0.743	0.555	0.279	0.048	0.024	0.019	0.016
12	2.88	2.73	1.32	0.800	0.601	0.288	0.044	0.022	0.017	0.015
14	1.55	1.50	0.95	0.668	0.538	0.288	0.051	0.026	0.020	0.017
16	1.22	1.19	0.87	0.657	0.538	0.292	0.052	0.026	0.020	0.017
18	1.14	1.13	0.89	0.681	0.555	0.293	0.051	0.026	0.020	0.016
20	1.25	1.23	0.91	0.589	0.465	0.276	0.058	0.030	0.023	0.019
22	1.31	1.29	0.99	0.630	0.472	0.271	0.057	0.030	0.023	0.019
24	1.10	1.09	0.90	0.619	0.469	0.269	0.059	0.031	0.024	0.020
26	0.93	0.92	0.81	0.600	0.462	0.265	0.059	0.032	0.025	0.020
28	0.80	0.79	0.72	0.572	0.452	0.264	0.061	0.032	0.025	0.021
30	0.69	0.68	0.64	0.537	0.438	0.260	0.063	0.034	0.027	0.022
40	1.08	1.08	1.00	0.816	0.612	0.265	0.049	0.026	0.021	0.020
50	1.24	1.24	1.16	0.964	0.731	0.280	0.041	0.021	0.019	0.015
60	1.25	1.24	1.16	0.961	0.724	0.272	0.041	0.022	0.019	0.017
70	1.14	1.14	1.06	0.876	0.659	0.253	0.045	0.027	0.024	0.022
80	0.92	0.92	0.85	0.689	0.512	0.216	0.054	0.036	0.023	0.031
90	1.45	1.45	1.35	1.105	0.832	0.295	0.033	0.016	0.013	0.011

Table 6. (Con't) Vertical profiles of spectral aerosol phase function $\mu_a(\varphi)$ and their parameters of asymmetry γ for Northern continental regions for λ= 0.530μm. Phase functions are normalized under the condition (12).

	φ							
h, km	120^0	130^0	145^0	150^0	160^0	170^0	180^0	γ
0	0.0087	0.0086	0.0132	0.0156	0.0155	0.0178	0.0228	15.71
1	0.0075	0.0078	0.0127	0.0161	0.0171	0.0199	0.0271	14.87
2	0.0098	0.0096	0.0123	0.0148	0.0241	0.0263	0.0296	11.71
3	0.0119	0.0117	0.0135	0.0151	0.0227	0.0343	0.0406	9.41
4	0.0123	0.0119	0.0137	0.0152	0.0217	0.0321	0.0380	9.48
5	0.0123	0.0121	0.0139	0.0153	0.0210	0.0297	0.0374	9.33
6	0.0124	0.0123	0.0142	0.0154	0.0202	0.0289	0.0358	9.32
7	0.0132	0.0131	0.0167	0.0159	0.0200	0.0272	0.0339	9.11
8	0.0140	0.0138	0.0154	0.0165	0.0201	0.0261	0.0326	8.58
9	0.0148	0.0146	0.0160	0.0170	0.0202	0.0260	0.0306	8.12
10	0.0151	0.0153	0.0166	0.0173	0.0196	0.0238	0.0285	7.83
11	0.0144	0.0142	0.0169	0.0169	0.0204	0.0269	0.0341	8.20
12	0.0140	0.0135	0.0157	0.0169	0.0223	0.0222	0.0249	8.86
14	0.0156	0.0155	0.0168	0.0175	0.0199	0.0239	0.0283	7.75
16	0.0156	0.0154	0.0167	0.0173	0.0196	0.0227	0.0269	7.81
18	0.0154	0.0153	0.0164	0.0172	0.0191	0.0223	0.0274	7.99
20	0.0172	0.0166	0.0170	0.0176	0.0196	0.0239	0.0304	6.92
22	0.0169	0.0165	0.0171	0.0178	0.0197	0.0253	0.0348	6.91
24	0.0177	0.0170	0.0178	0.0189	0.0197	0.0258	0.0352	6.63
26	0.0185	0.0178	0.0188	0.0197	0.0219	0.0265	0.0356	6.28
28	0.0195	0.0188	0.0200	0.0211	0.0231	0.0273	0.0354	6.01
30	0.0208	0.0203	0.0217	0.0227	0.0245	0.0288	0.0352	5.57
40	0.0177	0.0167	0.0218	0.0229	0.0259	0.0242	0.0271	6.80
50	0.0149	0.0154	0.0186	0.0201	0.0223	0.0211	0.0242	8.42
60	0.0163	0.0147	0.0212	0.0229	0.0254	0.0239	0.0273	7.75
70	0.0228	0.0239	0.0280	0.0299	0.0326	0.0315	0.0346	5.51
80	0.0322	0.0344	0.0396	0.0417	0.0453	0.0455	0.0473	3.72
90	0.0107	0.0113	0.0147	0.0162	0.0185	0.0167	0.0205	11.81

Table 7. Vertical profiles of spectral aerosol phase function $\mu_a(\varphi)$ and their parameters of asymmetry γ for Northern continental regions for λ=0.694 μm.
Phase functions are normalized under the condition (12).

	φ									
h, km	0^0	1^0	5^0	10^0	15^0	30^0	70^0	90^0	100^0	110^0
0	54.4	33.0	2.20	0.84	0.56	0.24	0.031	0.016	0.011	0.009
1	36.1	25.3	2.81	0.98	0.60	0.24	0.028	0.013	0.010	0.008
2	22.4	18.0	2.71	0.89	0.54	0.23	0.036	0.017	0.013	0.010
3	14.7	12.8	2.69	0.85	0.50	0.22	0.043	0.021	0.016	0.013
4	13.5	11.7	2.40	0.82	0.50	0.23	0.044	0.021	0.016	0.013
5	12.3	10.6	2.16	0.80	0.51	0.24	0.045	0.022	0.017	0.014
6	11.2	9.60	1.96	0.79	0.53	0.25	0.045	0.022	0.017	0.014
7	7.82	6.70	1.70	0.76	0.53	0.26	0.047	0.024	0.018	0.015
8	5.40	4.70	1.47	0.73	0.52	0.27	0.050	0.025	0.019	0.016
9	3.76	3.34	1.25	0.69	0.51	0.27	0.052	0.026	0.020	0.017
10	1.79	1.72	0.97	0.63	0.50	0.28	0.055	0.028	0.022	0.019
11	2.85	2.73	1.38	0.74	0.53	0.27	0.050	0.027	0.020	0.017
12	2.50	2.42	1.38	0.79	0.57	0.28	0.046	0.024	0.018	0.016
14	1.37	1.34	0.94	0.63	0.50	0.27	0.051	0.029	0.022	0.018
16	1.07	1.05	0.83	0.61	0.49	0.28	0.056	0.029	0.022	0.019
18	0.99	0.98	0.82	0.63	0.51	0.29	0.055	0.028	0.021	0.018
20	1.15	1.14	0.91	0.59	0.43	0.25	0.065	0.033	0.026	0.022
22	1.18	1.17	0.98	0.65	0.46	0.25	0.060	0.032	0.025	0.021
24	1.00	1.00	0.87	0.63	0.46	0.25	0.061	0.033	0.026	0.022
26	0.85	0.85	0.77	0.60	0.46	0.25	0.062	0.034	0.027	0.023
28	0.74	0.74	0.69	0.57	0.45	0.25	0.063	0.035	0.027	0.024
30	0.65	0.64	0.61	0.53	0.44	0.25	0.064	0.036	0.029	0.025
40	1.05	1.05	0.99	0.85	0.66	0.28	0.045	0.025	0.020	0.016
50	1.11	1.11	1.06	0.93	0.74	0.30	0.036	0.019	0.016	0.014
60	1.13	1.13	1.08	0.94	0.75	0.30	0.036	0.019	0.016	0.015
70	1.10	1.09	1.04	0.90	0.72	0.29	0.038	0.022	0.018	0.017
80	1.01	1.01	0.96	0.81	0.63	0.25	0.044	0.028	0.026	0.025
90	1.21	1.21	1.15	1.00	0.80	0.32	0.033	0.016	0.013	0.011

Table 7. (Con't) Vertical profiles of spectral aerosol phase function $\mu_a(\varphi)$ and their parameters of asymmetry γ for Northern continental regions for λ=0.694 μm. Phase functions are normalized under the condition (12).

	φ							
h, km	120^0	130^0	145^0	150^0	160^0	170^0	180^0	γ
0	0.008	0.009	0.015	0.018	0.018	0.021	0.030	12.97
1	0.008	0.008	0.014	0.019	0.019	0.024	0.034	13.74
2	0.009	0.010	0.013	0.016	0.029	0.032	0.033	10.87
3	0.012	0.011	0.014	0.017	0.027	0.045	0.052	8.91
4	0.012	0.012	0.014	0.016	0.026	0.041	0.049	9.02
5	0.013	0.012	0.015	0.017	0.025	0.037	0.046	8.49
6	0.013	0.013	0.016	0.016	0.024	0.035	0.045	8.69
7	0.014	0.014	0.016	0.017	0.023	0.033	0.041	8.25
8	0.015	0.015	0.017	0.018	0.023	0.031	0.040	7.87
9	0.016	0.015	0.018	0.019	0.023	0.030	0.037	7.44
10	0.016	0.016	0.017	0.019	0.022	0.027	0.032	7.14
11	0.015	0.015	0.016	0.018	0.023	0.031	0.041	7.63
12	0.014	0.014	0.018	0.019	0.023	0.025	0.028	8.20
14	0.017	0.017	0.018	0.019	0.022	0.026	0.032	6.79
16	0.017	0.017	0.018	0.019	0.022	0.025	0.030	6.90
18	0.017	0.016	0.020	0.018	0.021	0.024	0.030	7.21
20	0.020	0.019	0.020	0.021	0.024	0.029	0.039	5.83
22	0.019	0.019	0.021	0.022	0.025	0.031	0.045	5.91
24	0.020	0.019	0.022	0.023	0.025	0.031	0.044	5.72
26	0.021	0.020	0.023	0.024	0.026	0.032	0.043	5.44
28	0.022	0.022	0.024	0.025	0.027	0.032	0.041	5.20
30	0.022	0.023	0.025	0.027	0.028	0.033	0.040	4.95
40	0.017	0.018	0.021	0.022	0.024	0.024	0.026	7.34
50	0.014	0.014	0.017	0.017	0.018	0.019	0.021	9.51
60	0.014	0.015	0.018	0.019	0.020	0.020	0.023	9.15
70	0.017	0.019	0.022	0.023	0.024	0.025	0.028	7.52
80	0.025	0.028	0.032	0.034	0.036	0.037	0.039	4.78
90	0.010	0.011	0.013	0.014	0.014	0.015	0.017	12.68

Table 8. Vertical profiles of spectral aerosol phase function $\mu_a(\varphi)$ and their parameters of asymmetry γ for Northern continental regions for λ=0.860 μm.
Phase functions are normalized under the condition (12).

	φ									
h, km	0^0	1^0	5^0	10^0	15^0	30^0	70^0	90^0	100^0	110^0
0	43.4	30.9	2.68	0.87	0.55	0.22	0.029	0.013	0.011	0.009
1	27.1	21.3	3.13	1.05	0.61	0.23	0.027	0.012	0.010	0.008
2	17.2	14.8	3.03	0.97	0.55	0.22	0.035	0.017	0.013	0.011
3	11.3	10.4	2.96	0.94	0.51	0.21	0.041	0.021	0.016	0.013
4	10.7	9.79	2.69	0.89	0.52	0.22	0.043	0.022	0.016	0.013
5	9.94	9.00	2.43	0.86	0.52	0.23	0.044	0.022	0.017	0.014
6	9.15	8.23	2.18	0.83	0.52	0.24	0.045	0.023	0.017	0.014
7	6.63	5.99	1.88	0.80	0.52	0.25	0.048	0.024	0.018	0.016
8	4.75	4.33	1.60	0.76	0.51	0.25	0.050	0.026	0.020	0.017
9	3.41	3.15	1.35	0.71	0.50	0.26	0.053	0.027	0.021	0.018
10	1.68	1.63	1.01	0.62	0.47	0.26	0.057	0.030	0.024	0.020
11	2.54	2.47	1.46	0.76	0.52	0.25	0.051	0.026	0.021	0.018
12	2.27	2.22	1.45	0.81	0.56	0.26	0.048	0.024	0.019	0.018
14	1.28	1.26	0.95	0.63	0.47	0.26	0.057	0.030	0.024	0.020
16	0.99	0.98	0.81	0.59	0.46	0.27	0.056	0.031	0.024	0.021
18	0.91	0.90	0.78	0.60	0.48	0.27	0.052	0.030	0.023	0.020
20	1.10	1.09	0.93	0.63	0.43	0.23	0.063	0.035	0.028	0.024
22	1.12	1.12	0.98	0.69	0.48	0.23	0.061	0.033	0.028	0.023
24	0.95	0.95	0.86	0.66	0.48	0.24	0.061	0.034	0.027	0.023
26	0.83	0.82	0.77	0.63	0.48	0.24	0.061	0.035	0.027	0.024
28	0.72	0.72	0.68	0.59	0.47	0.24	0.061	0.036	0.028	0.025
30	0.63	0.63	0.60	0.54	0.45	0.25	0.062	0.035	0.024	0.026
40	0.99	0.98	0.94	0.83	0.68	0.29	0.042	0.023	0.019	0.017
50	0.95	0.95	0.92	0.82	0.70	0.32	0.039	0.019	0.016	0.014
60	0.97	0.97	0.94	0.84	0.70	0.32	0.037	0.019	0.015	0.014
70	0.96	0.96	0.93	0.83	0.70	0.31	0.038	0.020	0.017	0.015
80	0.97	0.97	0.93	0.82	0.68	0.29	0.039	0.023	0.021	0.020
90	0.86	0.86	0.83	0.75	0.64	0.32	0.043	0.021	0.016	0.014

Table 8. (Con't) Vertical profiles of spectral aerosol phase function $\mu_a(\varphi)$ and their parameters of asymmetry γ for Northern continental regions for λ=0.860 μm. Phase functions are normalized under the condition (12).

	φ							
h, km	120^0	130^0	145^0	150^0	160^0	170^0	180^0	γ
0	0.009	0.009	0.016	0.019	0.018	0.023	0.031	12.46
1	0.007	0.008	0.014	0.018	0.020	0.023	0.029	13.86
2	0.009	0.010	0.014	0.017	0.030	0.033	0.033	10.43
3	0.012	0.012	0.015	0.016	0.031	0.048	0.058	8.52
4	0.012	0.012	0.015	0.018	0.030	0.046	0.051	8.53
5	0.012	0.013	0.015	0.016	0.027	0.042	0.046	8.50
6	0.013	0.013	0.015	0.017	0.026	0.038	0.045	8.45
7	0.014	0.014	0.016	0.018	0.026	0.036	0.043	8.00
8	0.015	0.015	0.018	0.019	0.026	0.034	0.042	7.30
9	0.017	0.016	0.019	0.020	0.026	0.033	0.040	6.94
10	0.018	0.018	0.020	0.021	0.025	0.030	0.035	6.25
11	0.016	0.016	0.018	0.020	0.026	0.033	0.044	6.97
12	0.015	0.015	0.017	0.020	0.025	0.026	0.028	7.59
14	0.019	0.018	0.020	0.021	0.025	0.029	0.035	6.19
16	0.019	0.019	0.020	0.021	0.025	0.028	0.033	6.07
18	0.019	0.018	0.020	0.021	0.023	0.027	0.031	6.22
20	0.022	0.022	0.024	0.025	0.029	0.035	0.048	5.01
22	0.021	0.021	0.024	0.026	0.029	0.036	0.052	5.21
24	0.022	0.022	0.025	0.027	0.029	0.036	0.049	5.18
26	0.023	0.023	0.026	0.028	0.029	0.036	0.046	4.99
28	0.024	0.024	0.027	0.029	0.030	0.035	0.043	4.76
30	0.025	0.025	0.028	0.028	0.031	0.035	0.040	4.81
40	0.017	0.018	0.020	0.021	0.021	0.023	0.024	7.63
50	0.013	0.013	0.015	0.015	0.016	0.018	0.019	10.14
60	0.013	0.014	0.015	0.016	0.016	0.018	0.020	10.07
70	0.015	0.015	0.018	0.018	0.019	0.021	0.023	8.88
80	0.020	0.022	0.025	0.026	0.028	0.029	0.031	6.40
90	0.013	0.012	0.014	0.014	0.015	0.016	0.018	10.19

Average aerosol phase function for the total atmosphere $\mu_a^{aver}(\varphi)$ can be easily calculated according to relative weight of aerosol scattering at different altitudes:

$$\mu_a^{aver}(\varphi)=\sum\mu_a(\varphi, h)\ \sigma_a(h) / \sum \sigma_a(h)$$

where $\sigma_a(h)$ - coefficient of aerosol scattering at the height h. Its altitude dependency for wavelengths 0.530 μm, 0.694 μm and 0.860 μm is presented in Table 9 (Krekov and Rakhimov 1982).

Table 9. Altitude dependence of σ_a for Northern continental regions.

	σ_a		
h, km	0.530 μm	0.694 μm	0.860 μm
0	0.0972	0.0769	0.0652
1	0.0168	0.0142	0.0127
2	0.00842	0.00794	0.00609
3	0.00399	0.00333	0.00291
4	0.00231	0.00191	0.00162
5	0.00136	0.00110	0.000930
6	0.000807	0.000589	0.000548
7	0.000619	0.000454	0.000390
8	0.000491	0.000343	0.000282
9	0.000371	0.000259	0.000205
10	0.000546	0.000398	0.000285
11	0.000515	0.000391	0.000299
12	0.000335	0.000225	0.000177
14	0.000257	0.000178	0.000130
16	0.000107	0.000144	0.000102
18	0.000175	0.000125	0.0000900
20	0.0000661	0.0000481	0.0000334
22	0.0000143	0.0000118	0.0000085
24	0.0000118	0.0000081	0.0000059
26	0.0000082	0.0000056	0.0000040
28	0.0000057	0.0000036	0.0000028
30	0.0000039	0.0000026	0.0000019
40	0.0000012	0.00000095	0.00000074
50	0.00000050	0.00000044	0.00000037
60	0.00000056	0.00000046	0.00000039
70	0.00000061	0.00000044	0.00000043
80	0.00000180	0.00000130	0.00000105
90	0.00000080	0.00000063	0.00000050

5. Comparison of aerosol optical model for Siberia with other models

Based on the above discussion of vertical profiles of spectral aerosol phase function $\mu_a(\varphi)$ for Northern continental regions, average values of the asymmetry parameter γ of aerosol phase function for the total atmospheric height are about 12-13 for visible and 10-12 for near IR spectral ranges. These values are 15-30% greater than those used in the aerosol optical models for South Kazakhstan (Petelina 1997). In these models the average aerosol phase function for steppe areas near the Almaty region has the following spectral values for the asymmetry parameter:

λ=0.478 μm, γ=11.18;
λ=0.540 μm, γ=10.45;
λ=0.796 μm, γ=7.41.

This difference in γ can be initially explained by the presence of larger sized aerosol particles in the lower troposphere layer. This has been confirmed by recent airborne measurements of the concentration of aerosol submicron particles at different heights over Western Siberia (Panchenko *et. al.* 1996).

Spectral behavior of aerosol optical depth for Siberia differs from one in other continental regions such as South Kazakhstan (Almaty region), and the continental aerosol models WMO-1 and WMO-2 (Figure 10). The last two models were calculated from microphysical parameters recommended by World Meteorological Organization (WMO) (World Climatic Program 1986) and correspond to background rural conditions (WMO-continental 1) and desert (WMO-continental 2).

Average spectral values of aerosol optical depth in Siberia are significantly different from one for stepper region in South Kazakhstan near Almaty. This difference in spectral dependence of τ_a is caused by different types of aerosol particles in the lower troposphere originated from soil and vegetation, and also by different air mass circulation in these continental regions. Average values of aerosol optical depth in Siberia are larger than those in the WMO continental model-1, and smaller than in the WMO continental model-2. Also, their spectral dependence is different, especially in a range of wavelength 0.45-0.65 μm.

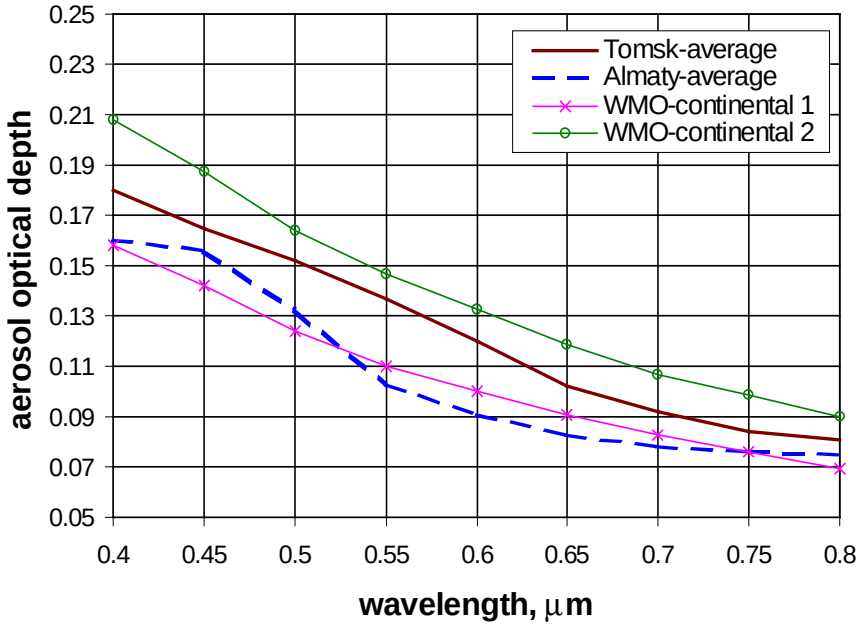

Figure 10. Spectral aerosol optical depth for Tomsk Oblast, South Kazakhstan (Almaty) region, and the continental aerosol models WMO-1 and WMO-2.

Standard atmospheric correction procedures assume the extraction of τ_a only for one wavelength (usually it is one in a spectral range 0.50-0.53 μm). For example, on the pixel per pixel basis (Zagolski and Gastellu-Etchegorry 1995), the approximation of τ_a for other wavelengths is done by using one of the known optical models. In this case, if atmospheric correction software is based on the global WMO optical model -1 for continental aerosols, then for Siberia the difference in spectral behavior of aerosol optical depth will lead to overestimation of $\tau_a(\lambda)$ in the spectral ranges 0.40-0.50 μm and larger than 0.55 μm. This overestimation, in turn, will cause the wrong restoration of the spectral signatures of objects on the ground surface, and may lead to significant errors in the interpretation of vegetation and soil condition. Therefore, using the aerosol optical models for determined geographic region provides more truthful interpretation of objects on the satellite images after the atmospheric correction procedure.

6. Conclusions

The regional aerosol optical model for Russian Siberia, which is necessary for the atmospheric correction of satellite images of the Earth surface in optical channels, is presented in this paper. This model is based on statistical experimental data measured in different areas of Siberia during the last 5-10 years. Our analysis of spatial, temporal and spectral behavior of aerosol optical and microphysical parameters in Siberia has found the following peculiarities:

- Aerosol size spectrum is similar in different areas of Siberia, and corresponds to 3-modes Whitby distribution.

- Spectral values of the asymmetry parameter of aerosol phase function indicate the presence of a significant amount of large and submicron aerosol particles in the lower troposphere.

- There was a decrease of up to 60% in the absolute values of aerosol optical depth from 1992 to 1995 years. This can be explained by the absence of aerosol particles in the atmosphere after the eruption of the volcano Pinatubo in 1991.

- Three periods in the daily behavior of aerosol optical depth exist:

    1. Morning period before 12:00 - characterized by low values with small variations

    2. Daytime period from 12:00 to 18:00 - characterized by continuous increase in aerosol optical depth

    3. Evening period, after 18:00 - characterized by a slight decreasing of aerosol optical depth.

- Spectral dependency of aerosol optical depth remains constant during the changes in relative air humidity.

- Spectral dependence of aerosol optical depth in Siberia is significantly different from other Northern continental regions.

Knowledge of these aerosol optical characteristics for Siberia makes it possible to correctly remove atmospheric effects from satellite images. This removal can be accomplished using either the pixel-per-pixel algorithm (which calculates the optical depth for one wavelength directly from the image, but models its spectral dependence and phase function) or the statistical approach (which assumes known average spectral, spatial and temporal atmospheric optical characteristics at the regional level).

7. References

Belan B.D., Zadde G.O. (1988) *Spectral transparency and aerosol extinction for USSR territory.* Tomsk. TF SB RAS. 180 p.

Deirmendjan D. (1969) Scattering of electromagnetic radiation by spherical polydisperse particles. 167 p.

Deschamps P.Y., Herman M., Lenoble J., Tanre D., Viollier M. (1980) *Atmospheric effects in remote sensing of ground and ocean reflectance*. International Remote Sensing of Atmospheres and Ocean. Edit. By A. Deepak. New York, pp.115-148.

Guschin G.P. (1988) *Methods, devices and results of measurement of atmospheric spectral transparency*. Sankt-Peterburg. 200 p.

Herman B.M., Browning S.R. (1975) *The effect of aerosols on the Earth-atmosphere albedo*. J. Atmos. Sci. Vol. 32. pp. 158-165.

Kabanov M.V., Sakerin S.M. (1996). *Variations of the atmospheric aerosol optical depth in the Tomsk region for several seasons during the period 1992-1995*. Optics of the Atmosphere and Ocean. Vol. 9, No 6. P. 727-736.

Kaufman Y.J., Sendra C. (1988) *Algorithm for automatic atmospheric correction for visible and near-infrared satellite imagery.* Int. J. Remote Sensing. Vol. 9, pp. 1357-1381.

Kimes D.S., Holben B.N. (1992) *Extracting spectral albedo from NOAA-9 AHVRR multiple view data using an atmospheric correction procedure and an expert system*. Int. J. Remote Sens. Vol. 13, No. 2, pp. 275-289.

Koutzenogii K.P. (1996) *Monitoring of Atmospheric Aerosols in Siberia*. Optics of the Atmosphere and Ocean. Vol. 9, No 6, pp.704-711.

Krekov G.M., Rakhimov R.F. (1982) *Optical-location models of the continental aerosol.* Novosibirsk. Nauka. 200 p.

Panchenko M.V., Terpugova S.A., Tumakov A.G. (1996) *Seasonal factors of the variability of submicron aerosol characteristics.* Atmos. Res. Vol. 41, pp. 203-215.

Petelina S.V. (1997) *Elaboration of regional optico-microphysical models of atmospheric aerosols.* PhD Thesis. Tomsk State University, 155 p.

Pkhalagov Ju.A., Uzhegov V.N., Shchelkanov N.N. (1996) *Aerosol attenuation of optical radiation in summer hazes of West Siberia.* Optics of Atmosphere and Ocean, No 6, pp. 720-726.

Pyaskovskaya-Fesenkova E.V. (1957) *Investigations of light scattering in the Earth atmosphere*. Moscow, 219 p.

Rahman H., Dedieu G. (1994) *SMAC: a simplified method for the atmospheric correction of satellite measurements in the solar spectrum*. Int. J. Remote Sensing. Vol. 15. No 1, pp. 123-143.

Rayleigh M. (1871) *On the scattering of light by small particles*. Philos. Mag. Vol. 140, No 4, pp. 447-454.

Singh S.M. (1992) *Fast atmospheric correction algorithm*. Int. J. Remote Sens. Vol. 13, No. 5, pp. 933-938.

Tverskoi N.N. (1962) *Course on meteorology*. Leningrad, 700 p.

Whitby K.T. (1975) *Modeling of atmospheric aerosol particles size distributions*. Progr. Rept. EPA-800971, 47 p.

World Climatic Program. World Meteorological Organization (1986). *A preliminary cloudless standard atmosphere for radiation calculations*. Boulder, Colorado, USA. 112p.

Zagolski F., Gastellu-Etchegorry J.P. (1995) *Atmospheric correction of AVIRIS images with a procedure based on the inversion of the 5S model*. Int. J. Remote Sensing. Vol. 16. No 16, pp. 3115-3155.